

OMAE2013-11356

DRAFT

**WAVE MODELLING FOR POTENTIAL WAVE ENERGY SITES AROUND THE OUTER
HEBRIDES**

Charles E Greenwood

Lews Castle Collage, University of Highlands and
Islands
Stornoway, Isle of Lewis, Scotland

Vengatesan Venugopal

University of Edinburgh
Edinburgh, Scotland

David Christie

Lews Castle Collage, University
of Highlands and Islands
Stornoway, Isle of Lewis,
Scotland

James Morrison

Lews Castle Collage, University
of Highlands and Islands
Stornoway, Isle of Lewis,
Scotland

Anre Vögler

Lews Castle Collage, University
of Highlands and Islands
Stornoway, Isle of Lewis,
Scotland

As further research into the environmental impact of WEC arrays advances, quantifying the initial resource by using finer scale maps will be essential. While this does provide advancements in mapping the initial resource the fine scale nature of the domain limits the use of these studies for potential site identification. This has left a gap for a broad scale approach where the regional resource distribution is assessed. This mid-scale model resolution will allow the assessment of multiple potential sites within a single model domain. Further benefits allow a more detailed spatial and temporal resolution than the national scale model while including other potential sites within the region.

For the present work Mike 21 SW model is chosen as this model can be applied to both deep and shallow water domains with finer scale grid spacing. This model enables the simulation of the build-up and transformation of wind and swell waves in the offshore and near shore environments. The SW model consists of two independent wave models, the fully spectral formulation and the directional decoupled parametric formulation. This study only considers the fully spectral formulation where the model formulation is based on the wave action conservation equation across a directional frequency spectra. This allows for model to account for wind induced waves, nonlinear wave interactions, white capping, bottom friction bathymetric refraction and shoaling, wave induced currents, and tidal variations. By using a cell centered finite volume technique the model applies an unstructured mesh grid to solve the wave action conservation equations within the model domain. This results in the model equating a solution using phase averaged equations. Further details on the SW model can be found in the user manual [5]. The methodology used for the wave modelling, calibration, validation and results obtained are detailed in the following sections. Considering the space limitations, detailed discussions for only significant wave heights are made.

METHODOLOGY

This study applies the Mike 21 SW model to the west coast of the Isle of Lewis in order to assess the spatial and temporal distribution of wave energy. The model domain was identified by including some of the potential development sites shown in Figure 1, where multiple sources of bathymetry data were used. The model boundary conditions were driven using time varying wave spectra from Siadar wave buoy. Further wave data was collected from a submerged AWAC (Acoustic Wave and Current profiler) and was used to calibrate and validate the wave model.

Computational Domain

The computational domain for this assessment focuses on the Voith Hydro Wavegen and the Aquamarine site locations (ref to Figure 1). This is due to the close proximity of the development sites and available bathymetry data. As Mike 21 SW allows the use of an unstructured mesh a nest domain can be created with varying resolution dependent on the level of

interest for any given location. The default bathymetry data used for this study consists of the GEBCO 08 data [11]. GEBCO 08 is an open source global bathymetry data set with a resolution of 30 arc seconds. This dataset was created using interpolated depth sounding and satellite gravity data. Due to the coarse nature of the data resolution this data has been applied to area where there is no other data or for relatively deep water region where wave-seabed interactions are minimal. A high resolution open source data created by Marine Scotland provides a 3m² dataset for the north coast of Lewis. This data exists for the entire North West coast of Lewis between approximately -20m and - 60m depth. Due to the scale of this dataset this data was filtered to 20m². A further dataset was collected by Aquamarine Power that covers the shallow waters behind their potential development site. This data extends from -5m to -15m with a resolution of less than 1m², due to the size of the dataset this was also filtered to 20m² resolution. All bathymetry datasets discussed above were converted to UTM-29 coordinates systems and to chart datum water levels.

The generation of the domain mesh uses separate mesh resolution steps that increase in detail towards the site of interest. The level reduced detail bathymetry for the South West of the model domain promotes the use of a coarse grid to enable the propagation of waves across the domain. The other coarse areas within the domain include regions of relatively deep water and non-vital areas. The reduced number of mesh nodes in these locations allows higher levels of detail in specific areas without increasing computational time requirements. For the mesh used in this study (shown in Figure 2) there are 2011 mesh elements with the fine scale mesh elements around the area of interest being approximately 100m apart.

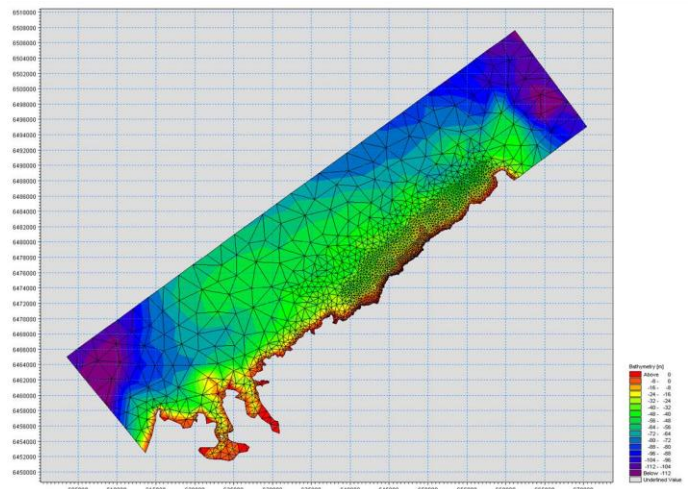


Figure 2. Nested computational domain where warmer colors indicate shallower water depths.

Boundary Input Parameters

The boundary conditions are driven by a Datawell MK III directional wave buoy (marked Siadar wave buoy) deployed in 60m depth at the location shown in Figure 1. The MK III wave

buoy provides directional wave spectral information x, y and z displacements and a magnetic compass [12]. The time series displacements are sampled at 1.28Hz for a 200 second period where an FFT (Fast Fourier Transformation) is used to create a frequency spectrum where 8 of these spectrums are combined to create a 30 minute spectral file where an additional 200 seconds is used for calculations and storage. The directional data is created by applying the Fourier series to the displacement data. This produces 9 Fourier components which are used to create 4 Fourier coefficients that in turn calculate direction and spread for each frequency bin. The spectral file provides a standard wave data file consisting of 64 frequency bins ranging from 0.025Hz to 0.58Hz and PSD (Power Spectral Density), direction, spread skew, and kurtosis for each frequency bin. A directional frequency spectrum is created combining the frequency and directional energy spectra as,

$$E(f, \theta) = E(f)D(f, \theta) \quad (1)$$

Where $E(f, \theta)$ is directional spectral density in frequency and direction, $E(f)$ is the energy frequency distribution, and $D(f, \theta)$ is the directional spreading function. As the wave buoy produces $E(f)$ in the spectral file the directional component must be generated mathematically. One of the simplest forms of directional distributions uses a normal or Gaussian distribution across $E(f)$ and can be shown as

$$D(f, \theta) = \frac{\exp\left[-\frac{1}{2}\left(\frac{\theta - \theta(f)}{\sigma}\right)^2\right]}{2\pi\sigma} \quad (2)$$

Where θ represents peak direction, $\theta(f)$ is the wave component direction with frequency ' f ' and σ is the wave spread. All directions including spreading should be calculated in radians for later use. To ensure the directional spectrum is compatible with Mike 21 SW the data must be filtered in the frequency domain to a linearly spaced distribution. This removes some of the lower frequency values resulting in 56 frequency bins ranging from 0.03-0.58Hz with a 0.01Hz spacing. For this study the spectral discretisation within the model will be run for 56 frequencies

The wave conditions were measured continuously for a year period from 1st December 2011 to the 30th November 2012, this provides 17571 data points at the model boundary. To effectively replicate the existing wave conditions within the domain a general idea of the wave climate should be identified. Figure 3 shows the wave direction with regards to percentage of occurrence and wave height for the year dataset plotted with 10° bins. It can be seen that the majority of waves propagate from 290° with a secondary peak originating from 30°. This level of variation in the incoming swell provides some challenges regarding the orientation of the main driving boundary. For this reason the North West boundary of the model domain is angled

and elongated to allow the propagation of waves through to the area of interest without experiencing interference from the other boundaries. Figure 3 also show 2 dominant peaks in wave direction, these peaks may potentially indicate the presence of bi-modal seas. With the focus of this study on identifying and

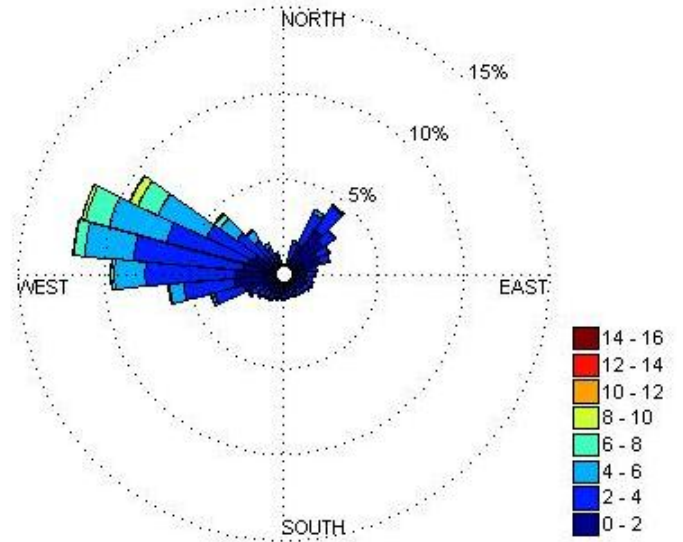


Figure 3. Wave direction of origin and percentage occurrence according to wave height in meters for a year.

quantifying the potential resource for the west coast of the Isle of Lewis the inclusions of bi-modal sea is likely to cause a significant impact on the results. This observation supports use of a fully directional frequency spectrum generated from measured data as model boundary conditions. Figure 4 shows a time series of the wave buoy measured wave heights and a weekly average. The duration of the measurements enable the observation of the seasonal change in wave height and the weekly averages. When the 30 minute and weekly averages are compared the winter months show a high levels of variation around the weekly average in contrast the summer.

When wave height and period are considered (see Table 1) and compared to a similar scatter table exhibited in Smith et al [10] for the Wave hub site, it can be seen that there are some differences in the annual wave climates. While the datasets from present study and Smith et al [10] do not cover the same time frame or region, a reasonable comparison can be drawn. When compared in the frequency domain the Hebridean wave buoy measured a higher occurrence of lower frequency waves with lower peak values. The level of variation recorded across the frequency domain was significantly higher in the Hebridean wave buoy than the one at the Wave hub location. When wave heights are considered the Hebridean wave buoy recorded a larger percentage of data points with significantly higher wave heights than the Wave Hub. The combination of lower wave frequencies (i.e., waves with longer wave lengths) and higher wave heights make the Isle of Lewis an attractive place for WEC array deployment; however the larger variation in wave conditions means WEC technologies need to be well proven

which controls energy dissipation through wave steepness. The process of calibrating a model to correlate with existing wave data is a trial and error process that is done over a series of model simulations.

In order to calibrate the wave model the data measured by the AWAC was used. The device was deployed in 16m depth of the North west coast of the Isle of Lewis (shown in Figure 1) on the 17th of January 2012. This device uses a combination of acoustic and pressure sensors to measure the wave climate. As this device requires manual data collection at the date of this study only 6 months of data had been collected. The AWAC data allows a direct comparison between the measured data and computational results for the same location. By applying a quantitative process of assessing the difference between the measured and modelled wave parameters a more accurate calibration process can be performed. This process uses simple statistical analysis to calculate the Bias, RMS Error, and the Scatter index shown below.

$$Bias = \frac{1}{N} \sum_{i=1}^N (x_i - y_i) \quad (3)$$

$$RMS\ error = \sqrt{\frac{1}{N} \sum_{i=1}^N (x_i - y_i)^2} \quad (4)$$

$$Scatter\ Index = \frac{RMS\ error}{\bar{x}} \quad (5)$$

Where N is the number of samples, x_i is measured dataset, y_i is the modeled dataset and \bar{x} is the mean of the measured dataset.

Due to the high resolution of wave data across the model and the computational time requirements, model calibration was conducted to a small time period. The smaller time series is located in the winter months where AWAC data is available. By using a relatively small time series from the winter period the seasonal variation can be accounted for. This time series was identified within March 2012 as it contains some of the larger recorded wave heights from the AWAC.

For calibrating the wave model the first stage of the calibration process uses the white capping parameter. This source term uses two parameters within an equation developed by Hasselman [13]. The main displacement coefficient (C_{ds}) that controls the magnitude of energy dissipation and a second frequency based term (δ) alters the energy dissipation across the frequency domain. As this term quantifies losses through wave steepness and breaking the effectiveness of this term are suited to calibrating larger scale models. If white capping is used to significantly increase energy loss within a small domain the value may extend beyond realistic values providing unreliable data. For relatively small domains where energy loss from white capping is negligible the main calibration parameter is bottom friction. This process changes the bottom friction parameters in an attempt to alter energy dissipation. The bottom friction source term is based on the equation by Battjes and Janssen

[14]. Within the SW model the sea bed interaction can be applied in several forms, this study uses the Nikuradse roughness (kn). This parameter is calculated based on hydrodynamic processes. The default parameters for the Nikuradse roughness is 0.08m. Figure 6 shows the effects of altering these parameters on the wave height over short time frame in March 2012. The default kn value of 0.04m simulates a higher wave height for the duration of the simulation. By increasing the bottom friction the rate of energy dissipation across the model is increased reducing the wave height at the AWAC location. This is shown in Figure 6 where the green dotted line more accurately represents the measured data.

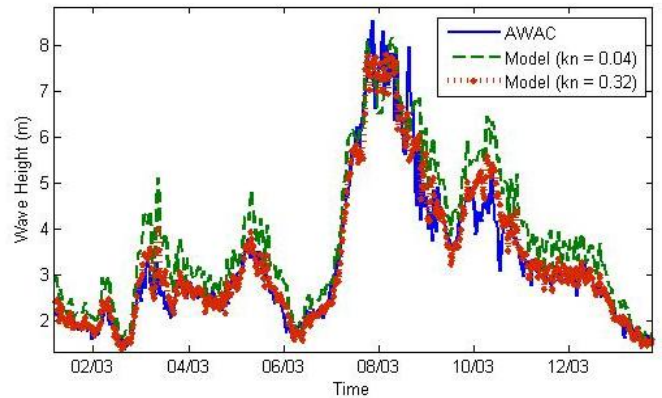


Figure 6. A direct comparisons between measured and modelled wave height data where bottom friction has been altered.

This qualitative method for assessing the relationship between measured and modelled data is limited. For the more fine scale calibrations simulation statistical analysis is implemented. When the scatter index is calculated for the default value of bottom friction the model shows an agreement of 0.22. When bottom friction is increased and the simulated wave height is shown to have a better agreement where the scatter index is 0.11. This value was then applied to the entire duration of the AWAC dataset where the model can be calibrated for seasonal variations in a more controlled approach. Figure 7 shows the model agreement between a parameter based model with the AWAC data with regards to bottom friction. A line of best fit has been calculated using the data points to interpolate between the data points. This suggests that optimal bottom friction value is between 0.3 and 0.35. As the bottom friction values approaches the optimum value the rate of change in the scatter index is reduced. To get the optimal model calibration coefficients the model runs a finite number of times. However, due to computational time limitations a compromise is made where a value within an acceptable error tolerance is taken and applied for the duration of the model. While the results for Figure 7 were based on a parameters based model the calibration values from this graph were taken and applied to the directional frequency spectra model.

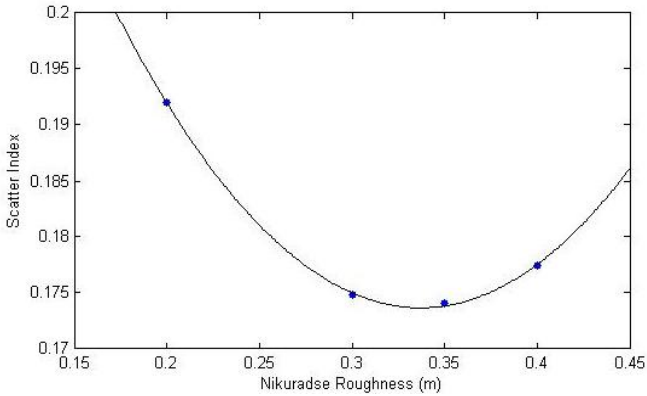


Figure 7. Model Scatter index with regards to Nikuradse roughness

Further model calibrations focus on the alteration of energy dissipation across the frequency spectra. This requires the manipulation of δ coefficient within the white capping parameter using the same technique used for adjusting the wave height. Figure 8 shows the agreement between AWAC and simulated data when the energy dissipation across the frequency is changed for the same time period as Figure 6. Due to the large storm event that occurred around the 8th of March 2012 the recorded wave period data contained large amounts of potential errors and was therefore removed. Figure 8 shows the simulated output to be over predicting the measured mean wave period. By reduction the δ coefficient an increased agreement with measured data can be observed. When the statistical method is applied to the short time period of existing data the $\delta = 0.5$ has a scatter index of 0.218 whereas the $\delta = 0.001$ has a scatter index of 0.17.

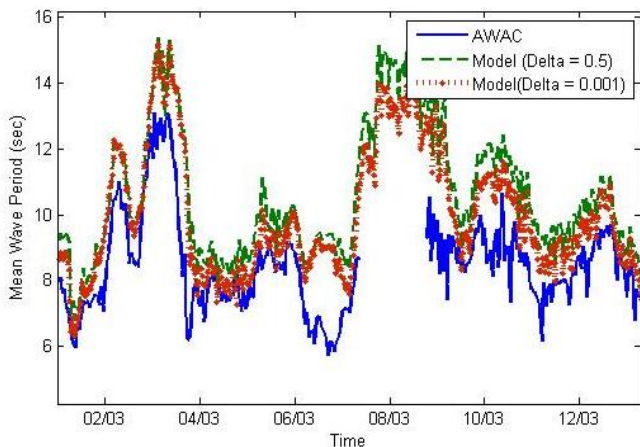


Figure 8. A direct comparison of model and measured data with regards to varying δ dissipation.

RESULTS AND DISCUSSION

Mike 21 SW model provides several outputs. To enable a simple comparison the results are compared using wave parameters. Due to the driving boundary using directional

frequency spectra and the importance of bi-model sea states on the location the resultant wave spectra should be assessed. The output parameters covered in Mike 21 SW model allow for the production of a time varying area plot, single point wave parameters and single point directional frequency wave spectra. These outputs will be used to compare the AWAC measured conditions with the simulated conditions for the AWAC location over a 6 month period. By calibrating the model for a short period of the dataset the rest of the data can be used as an independent validation point. Figure 9 shows wave height variation for the entire model and measured datasets. By observing the correlation between the dataset it is possible to state that there is a good agreement between measured and modeled data for the 6 months of measured data. The highlighted green segment indicates the period of calibration for the model, allowing all other data to be used for model validation purposes. When the wave height correlation is calculated for the extent of the measured data a scatter index of 0.13 is given, allowing the model to predict wave height within 13% for the AWAC location. When the variance coefficient is calculated for the mean wave period and peak wave period a scatter index of 0.14 and 0.07 respectively can be seen. For the most part the simulated results provide a good indication of the recorded wave parameters at the AWAC site. If the observed agreement between peak wave periods is considered the low value may be attributed to the high level of occurrence of dominant long period swell. Whereas the slightly higher correlation coefficients of the mean wave period may be caused by the lack of wind data as the modelled waves propagate across the model domain.

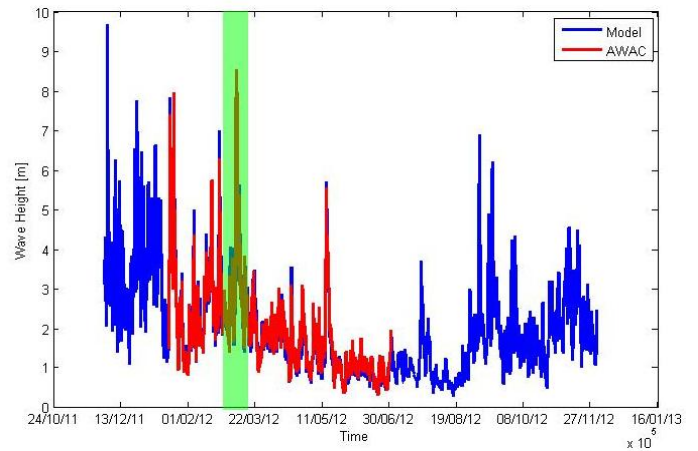


Figure 9. Time series of model and measured wave height with calibration period highlighted in green.

While the model is calibrated temporally to a single point in the model domain the distribution of wave energy can be assessed using spatial model outputs. To assess the spatial distribution of wave energy the results are presented in a time averaged format. While this may not result in the most accurate representation of the data for a specific site it allows an insight

into the energy distribution on the North West coast of Lewis. Figure 10 shows the results of the year long simulation calibrated using the March wave data. The coarse outer regions of the model domain have been excluded to allow a more detailed look at the area of interest. The results show a reduction in wave height as the waves propagate to shallower waters. Further variations in wave height along the coast can be seen around headlands and inlets. Regions of increased wave heights are shown to be located in areas of exposed outcrops and regions of reduced wave height are located in sheltered inlets. This spatial variation in average wave height is caused by bathymetric variations resulting in wave refraction. The two locations shown within Figure 10 Siadar 1 and 2 identify the locations of the initial stage for the WEC development for Voith Hydro Wavegen and Aquamarine Power respectively. The distribution of average wave heights along the coast provides important data for the positioning of these WEC arrays. The modeled data shows that the Siadar 1 site has a lower average wave height compared to the Siadar 2 site.



Figure 10. Average distribution of wave height in meters for the North West coast of Lewis.

As the model is based on series of equations it does not account for all environmental process, including reflections. The shallow near shore nature of the AWAC and potential WEC array locations means that there will be some reflection from the shoreline. As the model does not account for these reflections there will be some variations in the simulated wave spectra from the measured wave spectra. However, the comparison of the AWAC and model data show a good agreement indicating that while the model does not account for all parameters it still provides an a valid estimate of the shoreline wave parameters.

Currently as there are no available datasets within the model domain the spatial validation of the model result is unavailable. Due to the location of the AWAC and its proximity to the proposed WEC development sites the spatial degradation of the accuracy of the result is minimal; however the level of uncertainty surrounding the accuracy of the result increases with distance away from the temporally calibrated AWAC position.

Further work on quantifying the available wave resource for the west coast of Lewis is on-going. This will include the

comparison of modelled and measured wave spectra at the AWAC location, reassessing the spatial wave energy distribution using depth dependent parameters, quantifying and presenting near shoreline wave energy for the 10m depth contour of the area of interest and using the shoreline distribution results to identify possible future sites based on current WEC technologies.

Future research could also cover the development of a calibration procedure that utilizes directional frequency spectra to calibrated wave models. This process will include large amounts data for each model time step resulting in a more accurate model.

CONCLUSIONS

A calibrated and validated numerical wave model using Mike21 spectral wave module has been developed and applied to Outer Hebrides for the purpose of simulating near shore wave spectra and other wave parameters relevant to wave energy application. The model result shows a good agreement with the measured data from the Acoustic Wave and Current profiler (AWAC) showing a wave height correlation coefficient of 0.87 and mean wave period correlation coefficient of 0.86. The peak wave period correlation coefficient was calculated at 0.93. The agreement of the peak wave period value is expected to be lower than the mean wave period due to the high occurrence of dominant long period swell waves. This model provides a good representation of all wave parameters for the location of the AWAC. The variations observed within the wave period dimensions may be attributed to slight evolution of the wave spectra caused by local wind. More data which can be added to the model and may increase model accuracy includes the local effects of wind across the model domain.

The spatial distribution of wave heights across the area of interest sees a general increase in wave heights in deeper waters. When shallow water/near shore regions are considered increased wave heights can be seen around exposed outcrops while lower wave heights tend to be located in shelter inlets. When the proposed WEC array sites of Siadar 1 and Siadar 2 are compared, the surrounding bathymetric variation causes the focusing of waves towards the Siadar 2 resulting a higher average wave height.

ACKNOWLEDGMENTS

The author wishes to acknowledge the funding received from European regional development fund and the Hebridean Marine Energy Futures Project. Furthermore the author is grateful for the data and support from the Hebridean Marine Energy Futures Project partners and Lews Castle College.

REFERENCES

- [1] Scottish Government (2011) “2020 Route Map for Renewable Energy in Scotland,”
- [2] Aquamarine Power, www.aquamarinepower.com
- [3] Pelamis Wave Power, www.pelamiswave.com

- [4] Voith Hydro Wavegen, www.wavegen.co.uk
- [5] Danish Hydraulic Institute, (2011) "MIKE 21 Spectral Waves FM – Short Description," Hørsholm, Denmark.
- [6] Department of Business Enterprise and Regulatory Reform (BERR) (2008) "Atlas of UK Marine Renewable Energy Resource," www.renewables-atlas.info/downloads/documents/Renewable_Atlas_Pages_A4_April08.pdf.
- [7] The Crown Estate (2012) "UK Wave and Tidal Key Resource Areas Project Summary Report," www.thecrownestate.co.uk/media/355255/uk-wave-and-tidal-key-resource-areas-project.pdf.
- [8] Carbon Trust (2012) "UK Wave Energy Resource," www.carbontrust.com/media/202649/ctc816-uk-wave-energy-resource.pdf.
- [9] Venugopal, V. Smith, G.H. (2007) "Wave Climate Investigation for an Array of Wave Power Devices" Proc. 7th European Wave and Tidal Energy Conference, Porto, Portugal
- [10] Smith, H,C,M. Pearce, C. Millar, D,L. (2012) "Further Analysis of Changes in Nearshore Wave Climate: An enhanced case study for the Wave Hub site," *Renewable Energy*, 40, pp.51-64.
- [11] The General Bathymetric Charts of the Oceans (GEBCO), www.gebco.net.
- [12] Datawell "Datawell conventions for coordinate systems, angles, directions, Fourier transformations and other minus-signs,"
- [13] Hasselmann, K.(1974) "On The Spectral Dissipation of Ocean Wave due to White Capping," *Boundary Layer Meteorology*, 6(1-2), pp. 107-127.
- [14] Battjes, J, A., Janssen, J,P,F,M., (1978) "Energy loss and set-up due to Breaking of Random Waves," Proc. 16th International Conference on Coastal Engineering, pp. 569-587.